One- and Two-Photon Spectroscopy of Donor−Acceptor−Donor Distyrylbenzene Derivatives: Effect of Cyano Substitution and Distortion from Planarity

Stephanie J. K. Pond,[†] Mariacristina Rumi,[†] Michael D. Levin,[‡] Timothy C. Parker,[†] David Beljonne,[§] Michael W. Day,[‡] Jean-Luc Brédas,*[,†,§] Seth R. Marder,*[,†,||] and Joseph W. Perry*[,†,||]

Department of Chemistry, University of Arizona, Tucson, Arizona 85721, Center for Research on Molecular Electronics and Photonics, Université de Mons-Hainaut, B-7000, Mons, Belgium, Division of Chemistry and Chemical Engineering and Beckman Institute, California Institute of Technology, Pasadena, California 91125, and Optical Sciences Center, University of Arizona, Tucson, Arizona 85721

Received: August 7, 2002

The one- and two-photon spectroscopic properties of four symmetrically substituted donor−acceptor−donor distyrylbenzenes with either di-*n*-butyl- or diphenylamino donor groups and cyano acceptor groups are reported. It has been found that the position of the substitution of the electron-withdrawing cyano groups on the central phenylene ring as compared to the vinylene bond strongly affects the observed properties. In particular, the molecules with cyano substitution on the α-carbon of the vinylene linkage are characterized by weak fluorescence, short fluorescence lifetimes, and two-photon cross sections (δ) that are comparable to analogous molecules with no acceptor groups. In contrast, the molecules with acceptor substitution on the central phenylene ring are strongly fluorescent and have δ values roughly twice those of the vinyl-substituted molecules. These results are discussed in terms of the larger deviation of the conjugated backbone from planarity and the smaller distance between the donors and acceptors when the cyano groups are substituted on the vinylene carbon rather than the central phenylene ring.

Introduction

Molecular two-photon absorption processes are currently of considerable interest for applications including three-dimensional fluorescence imaging, photodynamic therapy, optical limiting, and three-dimensional microfabrication.[1−7] Recently, substantial efforts have been directed toward the identification of molecular design strategies for the development of chromophores with large two-photon absorption cross sections (δ). Such molecules offer the potential for greater sensitivity in various two-photon activated processes, which can allow lower laser intensities to be used for excitation, and reduced probability of optical damage. For example, fluorescent chromophores with large δ may allow for two-photon fluorescence imaging of biological samples with reduced photoinduced damage to the system under study. Various classes of two-photon chromophores have been investigated, including quasi-linear donor−acceptor quadrupolar molecules incorporating a variety of conjugated bridges,[8−13] bifluorene and polyfluorene systems,[14,15] various dipolar conjugated donor−acceptor molecules,[10] octupolar molecules,[16,17] multibranched structures,[18] and dendrimer systems.[19]

Previous studies in our laboratories have demonstrated that the magnitude of δ for quasi-linear donor−acceptor quadrupolar molecules can be correlated to the degree of intramolecular charge transfer upon excitation.[8,9,12] Conjugated molecules substituted with donor (D) and/or acceptor (A) groups in an essentially centrosymmetric pattern have been synthesized, and they exhibit two-photon cross sections at least 1 order of magnitude larger than the corresponding unsubstituted molecules. In particular, we have shown that, for molecules with general structure D−π−D (where π represents a conjugated bridge), δ increases and the position of the two-photon band is red-shifted with increasing chain length.[9] Moreover, for a given π bridge, conjugated D−A−D molecules can have larger δ values than D−π−D chromophores because the charge transfer between the terminal donor groups and the π system of the molecule is facilitated by the presence of the acceptor groups.[8] Similarly, molecules with the structural motif A−D−A can also exhibit large δ values.

One of the π bridges that we have examined is distyrylbenzene, which can be viewed as a segment of a poly(phenylenevinylene) (PPV) chain. It has been shown that PPV and its oligomers containing five rings exhibit a relatively planar conformation in the solid state.[20−22] When substituents are present on the chain, however, the conformation can be substantially nonplanar.[23−25] Theoretical calculations indicate that the degree of distortion of the π-backbone from planarity depends on the position of the substituents on the chain, on the vicinity of other substituents, and on the ability of the substituents to participate in hydrogen bonding interactions with other atoms or groups of the system.[26] The electronic coupling between donor and acceptor substituents in a molecule with a nonplanar backbone is effectively reduced due to the diminished overlap between the π orbitals of the conjugated bridge. This may impact the two-photon absorption cross section because it could modify the change in the charge distribution between the ground and two-photon excited state. On the other hand, it has recently been reported, on the basis of quantum chemical calculations, that torsional distortion from planarity of a

* To whom correspondence should be addressed. E-mail: (for J.W.P.) jwperry@u.arizona.edu, (for J.L.B.) jlbredas@u.arizona.edu, (for S.R.M.) smarder@u.arizona.edu.
[†] Department of Chemistry, University of Arizona.
[‡] California Institute of Technology.
[§] Université de Mons-Hainaut.
[||] Optical Sciences Center, University of Arizona.

10.1021/jp0267104 CCC: $22.00
Published on Web 11/02/2002

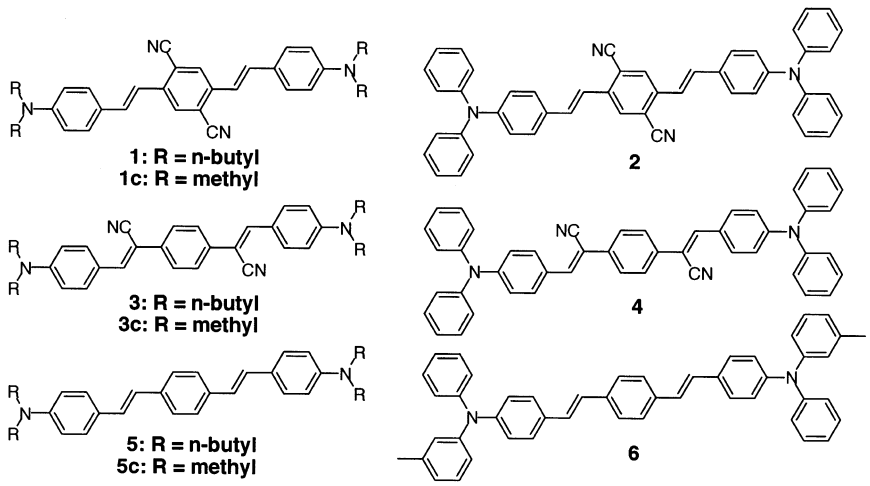

Figure 1. **1**−**4**: Molecular structure of the D−A−D compounds studied in this work. **5**-**6**: D−π−D compounds included for comparison. **1c**, **3c**, **5c**: Model compounds used for quantum chemical calculations.

4-quinopyran donor−acceptor molecule can lead to enhancement of two-photon absorption through increased charge localization and tuning into a "triple" resonance condition.[27] Additionally, calculations on bis-acceptor-substituted (A−π−A) difuranonaphthyl chromophores indicate that δ is relatively insensitive to torsions of the terminal acceptor group up to angles of about 50° and then decreases rapidly with increasing torsion angle.[28] Moreover, the position of the substituents can itself affect the two-photon properties of the chromophores because of the different lengths over which the intramolecular charge transfer can take place.

In this paper, we report on the effect of the position of the acceptor substitution and the distortion from planarity on the one- and two-photon optical properties of a series of D−A−D molecules (Figure 1). We have investigated four molecules with distyrylbenzene as the conjugated bridge, diphenyl- or di-*n*-butylamino groups as terminal electron donors, and cyano groups as acceptors substituted either on the central phenylene ring or on the α-carbon of the vinyl bond. As will be discussed in detail below, the molecules with the cyano substitution on the vinyl bond are substantially more distorted from planarity, as determined from X-ray crystallography, and have a smaller D−A distance than those substituted on the central phenylene. In the sections that follow, we will address: (1) the one- and two-photon spectroscopy, (2) the analysis of the vibronic band shapes of the absorption and fluorescence spectra, (3) the fluorescence quantum yields and lifetimes, (4) the ordering of the low-lying excited states, and (5) the two-photon cross sections for the molecules examined. Quantum chemical calculations have been performed to provide insight into the effect of positional substitution and torsional distortion on the two-photon properties.

Experimental Section

(i) Synthesis. The molecular structures of compounds **1**−**4** discussed in this paper are shown in Figure 1. Synthetic details and characterization data for these molecules are reported below (see Scheme 1).

1,4-Bis(diethylphosphorylmethyl)-2,5-dicyanobenzene (**P-1**),[29] 2,5-dicyano-1,4-bis(triphenylphosphonium)benzene dibromide (**P-3**),[30,31] and 4-(*N*,*N*-diphenylamino)benzaldehyde (**P-4**)[32] were synthesized according to literature procedures. 4-(*N*,*N*-Di-*n*-butylamino)benzaldehyde (**P-2**) and 1,4-bis(cyanomethyl)benzene (**P-5**) were purchased from Aldrich and used as received.

SCHEME 1: Synthetic Scheme for Molecules 1−4

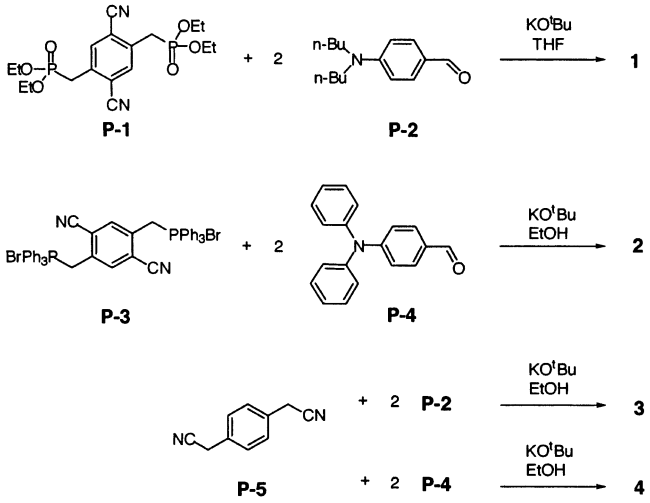

^{1}H NMR spectra were recorded on a General Electric QE−300 FT NMR, Varian Unity Plus-500, or a Bruker AM-250 MHz NMR spectrometer using the residual proton resonance of the solvent or tetramethylsilane as the internal standard. Chemical shifts are reported in parts per million (ppm). When peak multiplicities are given, the following abbreviations are used: s, singlet; d, doublet; t, triplet; q, quartet; dd, doublet of doublet; quin, quintet; sx, sextet; m, multiplet; b, broad. ^{13}C NMR spectra were recorded as proton-decoupled spectra or as attached proton test (APT) spectra on a QE-300 or Varian Unity Plus-500 using the carbon signal of the deuterated solvent as the internal standard. Fast atom bombardment (FAB) mass spectra were performed at the University of California, Riverside, or at the University of California, Los Angeles, Mass Spectrometry Facilities. Electron impact mass spectra (EIMS) were performed on Finnigan-MAT CH-5 and 311-A spectrometers at the California Institute of Technology Mass Spectrometry Facility. Elemental analyses were performed by Atlantic Microlab, Inc., Norcross, GA, or Desert Analytics, Tucson, AZ. Flash chromotography was performed with EM Science 37−75 μm silica gel. Analytical thin-layer chromatography was performed on EM Science silica plates with F-254 indicator and the visualization was accomplished by a UV lamp or using the molybdic acid stain mixture. All solvents and reagents were used as obtained from commercial sources unless otherwise mentioned.

*2,5-Dicyano-1,4-bis[2-(4-(di-n-butylamino)phenyl)vinyl]benzene (**1**).* Potassium *tert*-butoxide (359 mg, 3.2 mmol) was added to a solution of **P-1** (676 mg, 1.6 mmol) and **P-2** (747 mg, 3.2 mmol) in tetrahydrofuran (15 mL) at 0 °C. After 30 min, distilled water (75 mL) was added to the reaction mixture and a precipitate formed. The product was extracted with dichloromethane and separated by column chromatography on silica gel using a hexane/dichloromethane eluent (1:4), yield 729 mg (79%). ^{1}H NMR (500 MHz, $CDCl_3$), δ: 7.96 (s, 2H), 7.45 (d, $J = 9.0$ Hz, 4H), 7.19 (d, $J = 15.5$ Hz, 2H), 7.10 (d, $J = 16.0$ Hz, 2H), 6.65 (d, $J = 9.0$ Hz, 4H), 3.33 (t, $J = 7.5$ Hz, 8H), 1.61 (m, 8H), 1.38 (m, 8H), 0.98 (t, $J = 7.3$ Hz, 12H). ^{13}C NMR (125 MHz, $CDCl_3$), δ: 148.90, 138.49, 134.35, 128.92, 128.76, 122.60, 117.24, 116.29, 113.87, 111.44, 50.74, 29.40, 20.30, 14.00. Anal. Calcd for $C_{40}H_{50}N_4$: C, 81.87; H, 8.59; N, 9.55. Found: C, 81.99; H, 8.72; N, 9.49.

*2,5-Dicyano-1,4-bis[2-(4-(diphenylamino)phenyl)vinyl]benzene (**2**).* Potassium *tert*-butoxide (1.122 g, 10.0 mmol) was added over 15 min to a solution of **P-3** (3.354 g, 4.0 mmol) and **P-4** (2.733 g, 10.0 mmol) in ethanol (100 mL), and the resulting solution was refluxed for 1 h. A precipitate formed upon cooling of the solution to room temperature. It was filtered and recrystallized from a dichloromethane solution upon slow diffusion of petroleum ether, yield 1.354 g (51%). ^{1}H NMR (500 MHz, $CDCl_3$), δ: 7.99 (s, 2H), 7.43 (d, $J = 8.7$ Hz, 4H), 7.29 (m, 8H), 7.23 (d, $J = 4.0$ Hz, 4H), 7.14 (m, 8H), 7.09 (m, 4H), 7.05 (d, $J = 8.7$, 4H). ^{13}C APT NMR (75 MHz, $CDCl_3$), δ: 149.04 (C), 147.01 (C), 138.70 (C), 134.26 (CH), 129.43 (CH), 129.35 (CH), 128.88 (C), 128.35 (CH), 125.13 (CH), 123.77 (CH), 122.29 (CH), 119.50 (CH), 116.79 (C), 114.57 (C). FAB MS: *m*/*z* 667.3 ($[M + H]^+$, 100), 499.1 ($[M - NPh_2]^+$, 14). Anal. Calcd for $C_{48}H_{34}N_4$: C, 86.46; H, 5.14; N, 8.40. Found: C, 86.39; H, 5.19; N, 8.36.

*1,4-Bis[1-cyano-2-(4-(di-n-butylamino)phenyl)vinyl]benzene (**3**).* Potassium *tert*-butoxide (50 mg, 0.45 mmol) was added to a solution of **P-5** (0.625 g, 4.0 mmol) and **P-2** (2.00 g, 10.0 mmol) in ethanol (50 mL), and the resulting solution was refluxed for 2 h. The solvent was removed on a rotary evaporator, and the residue was separated by column chromatography on silica gel with dichloromethane and recrystallized from an ether/hexane mixture, yield 0.61 g (26%). ^{1}H NMR (250 MHz, $CDCl_3$), δ: 7.83 (d, $J = 9.0$ Hz, 4H), 7.63 (s, 4H), 7.39 (s, 2H), 6.64 (d, $J = 9.0$ Hz, 4H), 3.32 (t, $J \sim 7$ Hz, 8H), 1.59 (b quin, $J \sim 7$ Hz, 8H), 1.36 (sx, $J \sim 7$ Hz, 8H), 0.96 (t, $J = 7.2$ Hz, 12H). ^{13}C APT NMR (75 MHz, $CDCl_3$), δ: 149.83 (C), 142.23 (CH), 135.01 (C), 131.68 (CH), 125.61 (CH), 120.62 (C), 119.50 (C), 111.19 (CH), 102.67 (C), 50.78 (CH_2), 29.38 (CH_2), 20.30 (CH_2), 13.98 (CH_3). FAB MS: *m*/*z* 587.4 ($[M + H]^+$, 100), 530.3 ($[M - C_4H_9]^+$, 18), 487.3 ($[M - C_4H_9 - C_3H_7]^+$, 16). EIMS: *m*/*z* 587, 544, 501, 250, 218. FAB HRMS ($CHCl_3$−NBA): *m*/*z* 586.4057 ($[M]^+$ $C_{40}H_{50}N_4$ requires 586.4035). Anal. Calcd for $C_{40}H_{50}N_4$: C, 81.87; H, 8.59; N, 9.55. Found: C, 81.77; H, 8.63; N, 9.58.

*1,4-Bis[1-cyano-2-(4-(diphenylamino)phenyl)vinyl]benzene (**4**).* Potassium *tert*-butoxide (50 mg, 0.45 mmol) was added to a solution of **P-5** (0.625 g, 4.0 mmol) and **P-4** (2.73 g, 10.0 mmol) in ethanol (300 mL), and the resulting solution was refluxed for 2 h. The ethanol was removed on a rotary evaporator, and the residue was separated by column chromatography on silica gel. The fraction was eluted with a 1:1 mixture of dichloromethane and petroleum ether and was evaporated. The residue was recrystallized from benzene, yield 2.50 g (94%). ^{1}H NMR (500 MHz, $CDCl_3$), δ: 7.78 (d, $J = 9.0$ Hz, 4H), 7.67 (s, 4H), 7.45 (s, 2H), 7.30 (t, $J = 7.5$ Hz, 8H), 7.15 (d, $J = 7.5$ Hz, 8H), 7.12 (t, $J = 7.5$ Hz, 4H), 7.03 (d, $J = 9.0$ Hz, 4H). ^{13}C NMR (125 MHz, CD_2Cl_2), δ: 150.60, 146.93, 142.18, 142.13, 135.52, 131.18, 129.99, 126.58, 126.43, 126.28, 124.95, 120.85, 118.85, 106.94. EIMS: *m*/*z* 666 ($[M]^+$, 100), 586 (6), 333 (18), 258 (20), 218 (5), 131 (5), 69 (15). FAB HRMS ($CHCl_3$−NBA): *m*/*z* 666.2786 ($[M]^+$ $C_{48}H_{34}N_4$ requires 666.2783). Anal. Calcd for $C_{48}H_{34}N_4$: C, 86.46; H, 5.14; N, 8.40. Found: C, 85.58; H, 4.99; N, 8.54.

(ii) X-ray Crystallography. Single-crystal X-ray diffraction data were collected for compounds **2** and **4**. Single crystals were grown at room temperature by slow diffusion of petroleum ether vapor into a solution of compound **2** in chloroform or **4** in dichloromethane in a closed container. Crystal structure determinations were performed on a CAD-4 diffractometer using Mo Kα radiation ($\lambda = 0.71073$ Å) at the California Institute of Technology X-ray Crystallography Laboratory. The structures were solved using direct methods with SHELXS-86,[33] and the parameters for the non-hydrogen atoms were refined with full-matrix least-squares procedures using SHELXL-93.

(iii) Spectroscopic Measurements. All spectroscopic measurements were performed on toluene solutions (spectrophotometric grade, from Aldrich), unless otherwise noted. UV−visible absorption spectra were recorded on a Hewlett-Packard 8453 diode array spectrophotometer. Extinction coefficients, ϵ, were measured on multiple solutions obtained by dilution of two independent stock solutions. Corrected fluorescence spectra were collected on a Spex Fluorolog-2 spectrofluorometer. Quantum yields, η, of dilute solutions were determined using 9,10-bis(phenylethynyl)anthracene in cyclohexane ($\eta = 1.00$), as the reference compound.[34] Electrochemical potentials in tetrahydrofuran were obtained by cyclic voltammetry, as described previously,[9] and are reported relative to ferrocenium/ferrocene.

Fluorescence lifetimes were measured using the time-correlated single photon counting method.[35] The molecules were excited at 305 nm using the frequency doubled output of a picosecond dye laser and the fluorescence was detected perpendicular to the excitation beam after passing through an analyzer set at the magic angle. The instrumental response function full width at half-maximum was ≈90 ps. The details of the experimental setup and method of analysis of the data have been described previously.[36]

The two-photon absorption cross sections were determined by the two-photon induced fluorescence method[37] using both femtosecond and nanosecond pulsed lasers as excitation sources. The reference standards (r) used in the measurement of δ were fluorescein (in water, pH 11) and coumarin 307 (in methanol), whose two-photon properties have been well characterized in the literature.[37] At each wavelength, δ for a sample (s) is given by

$$\delta_s = \frac{S_s \eta_r \Phi_r C_r}{S_r \eta_s \Phi_s C_s} \delta_r \qquad (1)$$

where S is the detected two-photon induced fluorescence signal, η is the fluorescence quantum yield, and C is the concentration of the chromophore.[9] Φ is the collection efficiency of the experimental setup and accounts for the wavelength dependence of the detectors and optics as well as the difference in refractive indexes between the solvents in which the reference and sample compounds are dissolved. The measurements were conducted in a regime where the fluorescence signal showed a quadratic dependence on the intensity of the excitation beam, as expected for two-photon induced emission.[38]

Nanosecond pulse experiments were performed using the experimental setup as described previously,[9] in which the excitation source was a Nd:YAG pumped optical parametric oscillator (Quanta-Ray, MOPO 730) with a 5 ns pulse duration and 10 Hz repetition rate, tunable over the wavelength range of 430−700 and 730−2000 nm. The concentrations of the solutions were $\approx 1 \times 10^{-4}$ M for both the sample and reference compounds. The data reported were averaged over 200 pulses at each wavelength. The two-photon cross sections were also measured using a Ti:Sapphire laser (Spectra-Physics, Tsunami) as the excitation source. This laser generates ca. 85 fs pulses at a repetition rate of 82 MHz in the wavelength range of 710−1000 nm. The optical setup has been described previously.[29] The concentration of the solutions were $\approx 2 \times 10^{-5}$ M for **3** and **4** and $\approx 1 \times 10^{-6}$ M for **1**, **2**, and the reference compounds. The fluorescence collection was performed at the same detection wavelength for reference and sample compounds (535 nm). The output signal was averaged for 60 s for each excitation wavelength.

(iv) Quantum Chemical Calculations. Quantum chemical calculations have been performed using the same methodology described in our previous papers.[8,9] With AM1[39] optimized geometries, the energies and transition dipole moments for singlet excited states were calculated by combining the intermediate neglect of differential overlap (INDO) Hamiltonian[40] with a multireference double-configuration interaction (MRD-CI) scheme (using the Ohno−Klopman potential). The imaginary part of the second hyperpolarizability, $\gamma(-\omega;\omega,\omega,-\omega)$, which is proportional to the two-photon cross section at the excitation frequency ω, $\delta(\omega)$, was calculated using the sum-over-states expressions.[41] The damping factor was set to 0.1 eV in all cases. The calculations were performed on the model compounds **1c** and **3c** (Figure 1) which have terminal dimethylamino donor groups and cyano acceptor groups substituted on either the central phenylene ring or the vinylene α-carbon, respectively.

Results and Discussion

(i) Synthesis. Molecule **1** was synthesized using Horner−Emmons chemistry with diphosphonate (**P-1**) and 4-(*N*,*N*-di-*n*-butylamino)benzaldehyde (**P-2**) (Scheme 1). Molecule **2** was synthesized by a Wittig reaction between the diphosphonium salt **P-3** and 2.5 equiv of (diphenylamino)benzaldehyde **P-4**. Last, molecules **3** and **4** were synthesized via a Knoevenagel condensation between 1,4-bis(cyanomethyl)benzene (**P-5**) and the substituted benzaldehyde **P-2** and **P-4**, respectively.

(ii) Molecular Structure in the Crystal. The complete set of crystallographic data for **2** and **4**, atomic positions, and molecular geometric parameters are included as Supporting Information. Selected structural data are reported in Table 1. Analysis of the data and inspection of Figure 2 indicate that the central distyrylbenzene core of both molecules are distorted from planarity in the solid state, but molecule **4** is distorted to a much larger extent. In the discussion that follows, we will use P_C to indicate the central phenylene ring and P_L and P_R to refer to the outer left and right rings, respectively, in the distyrylbenzene backbone (see Figure 2). In molecule **4**, the angle between the planes defined by the rings P_L and P_C is about 72°. This large distortion from planarity is partly due to the steric hindrance between the cyano groups and the hydrogens on the P_C and P_L rings. The dihedral angle C0−C3−C4−C9 is −36°, and the dihedral angle C0−C3−C2−C1 is −4°, indicating that the cyano group (C0, N0) lies in approximately the same plane as the vinylene linkage but not in the plane of any of the rings. This strong distortion of the π-backbone has been

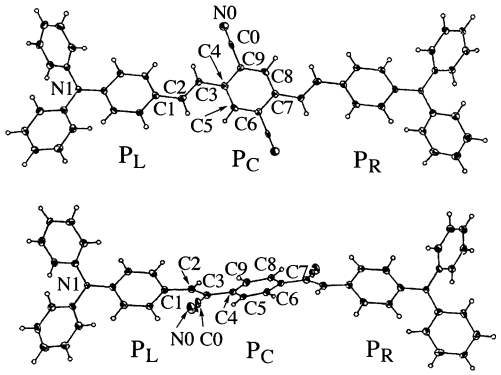

Figure 2. ORTEP plots with 50% probability ellipsoids (non-hydrogen atoms) from X-ray data for **2** (top) and **4** (bottom).

TABLE 1: Selected Bond Lengths, Angles, and Dihedral Angles for Molecules 2 and 4, As Obtained from X-ray Crystallographic Data[a]

	molecule **2**	molecule **4**
	Distances (Å):	
C1−C2	1.463	1.462
C2−C3	1.328	1.353
C3−C4	1.467	1.478
C0−C3		1.440
C0−C9	1.451	
N0−C0	1.139	1.137
N1−C0	8.831	6.537
N1−C3		6.623
N1−C9	9.040	
	Dihedral Angles (deg):	
C1−C2−C3−C4	+179.5	−176.4
C2−C3−C4−C9	−155.7	+136.8
C0−C9−C4−C3	+2.8	
C0−C3−C2−C1		−3.7
C0−C3−C4−C9		−36.3
	Angles between Planes (deg):	
P_L-P_C	≈43	≈72

[a] See Figure 2 for the numbering and labeling scheme.

observed for other cyano-substituted distyrylbenzenes.[23,24] In the case of molecule **2**, the cyano groups lie in the plane defined by P_C, and there appears to be less distortion in the π-backbone with an angle between the planes of P_L and P_C of 43°. The vinylene linkage (atoms C1, C2, C3, and C4) is approximately planar. Another parameter of interest with respect to electronic and optical properties is the donor−acceptor distance, defined here as the distance between the atom N1 of the donor group and C0 of the acceptor group, which is 6.5 Å in **4** and 8.8 Å in **2**, and thus is 2.3 Å shorter in **4** than in **2**. Although these data are for the molecules in the solid state, it is expected that even in solution the effect of steric hindrance due to the cyano substitution will be greater in the vinyl-substituted molecules than in phenylene-substituted molecules, causing **3** and **4** to be more twisted than **1** and **2**.

(iii) One- and Two-Photon Spectroscopy. The one-photon absorption, fluorescence, and two-photon induced fluorescence excitation spectra for molecules **1**−**4** are displayed in Figure 3. The corresponding spectroscopic parameters are reported in Table 2. Data for two molecules with no cyano substituents, **5** and **6**, have been included for comparison purposes.[8,9]

One-Photon Electronic Absorption Spectroscopy. The one-photon absorption maximum ($\lambda_{abs}^{(1)}$) is shifted to longer wavelength when cyano groups are bound to the π-backbone, as expected for substitution with an electron-accepting group. Specifically, the red shift for **1** and **2** compared to **5** and **6** (80 and 64 nm, respectively) is greater than for the molecules where

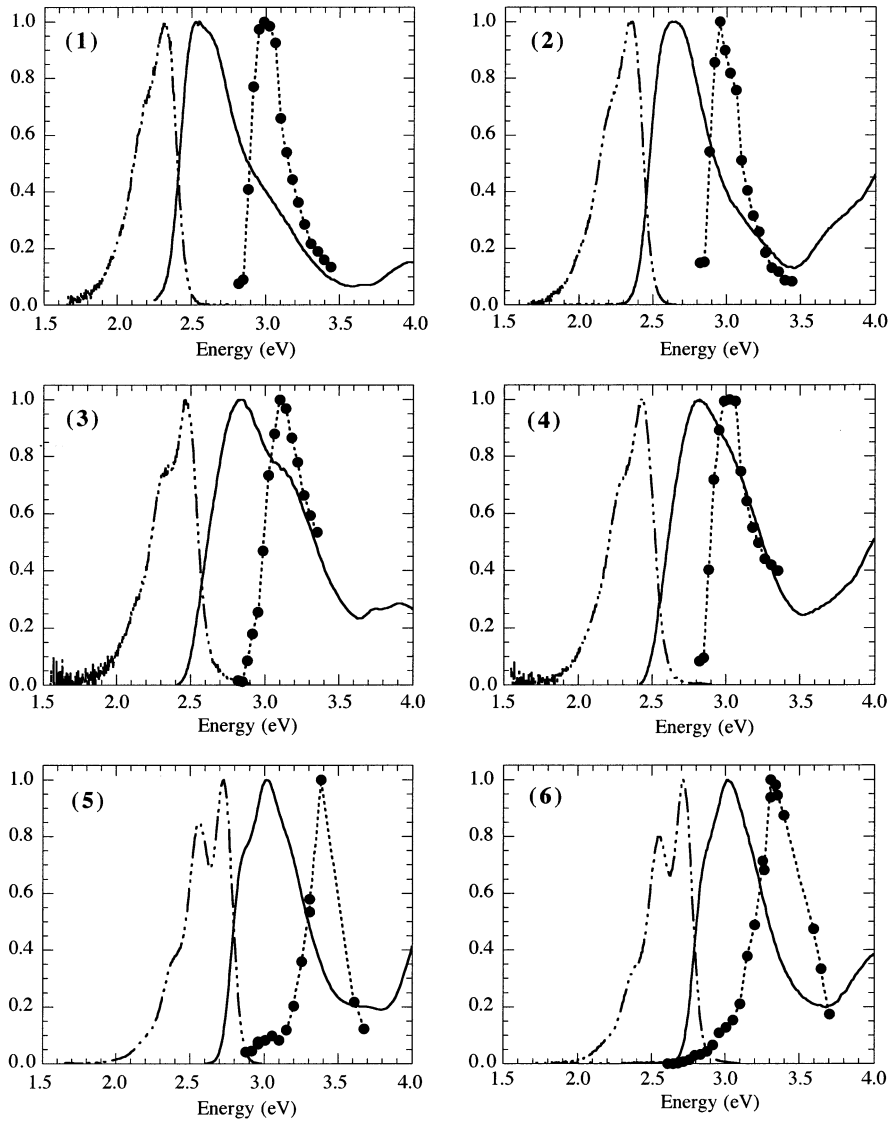

Figure 3. Normalized one- and two-photon spectra of D−A−D molecules **1**−**4** and D−π−D molecules **5** and **6**. The solid line is the one-photon absorption spectrum; the dashed line is the one-photon fluorescence spectrum (excitation wavelengths used are 430 nm for **1** and **2**, 420 nm for **3** and **4**, 400 nm for **5**, and 350 nm for **6**). The two-photon induced fluorescence excitation spectra (femtosecond measurements using fluorescein as reference) are represented by solid circles (the dotted line is only a guide to the eye). The two-photon spectra are plotted as a function of the total transition energy (twice the photon energy).

the cyano substitution is on the vinyl groups (≈30 nm for **3** and **4**). For molecules **3** and **4**, as well as **5** and **6**, the value of $\lambda_{abs}^{(1)}$ is not strongly affected by the type of substituent on the terminal amino group (dibutyl or diphenyl), as observed previously for distyrylbenzenes.[9] We have also reported that, in the case of molecules with a stilbene bridge, diphenylamino substitution was observed to cause a red shift in the absorption maximum relative to compounds with dibutylamino substituents.[42] In contrast, there is a 15 nm shift to the blue in $\lambda_{abs}^{(1)}$ of **2** with respect to **1**. However, the intensity distribution of the vibronic components in the absorption spectra of **1** and **2** is different.

Franck−Condon Band Shape Analysis. To compare more quantitatively the shapes of the absorption bands of these compounds, we performed a Franck−Condon analysis of the absorption (and fluorescence) spectra of molecules **1**−**6**. According to the Franck−Condon (F−C) principle, for the transition between the ground (g) and first excited (e) states of a molecule, the intensity of the $v'-v''$ vibronic component of the absorption band (v' and v'' represent the vibrational quantum numbers for states g and e, respectively) is proportional to the square of the transition dipole moment between the two states, M_{ge}, and the square of the overlap integral between the vibrational wave functions of the initial and final states, $\langle v'|v''\rangle$.[43] It can be shown that, for each vibrational mode and for $v' = 0$, the overlap integral can be expressed as

$$\langle 0|v''\rangle = \{\exp(-S/2)S^{v''/2}\}/(v''!)^{1/2} \qquad (2)$$

Equation 2 is derived under the assumption that the potential energy surfaces for the ground and excited states are parabolic, are characterized by the same vibrational frequency (ω_v), and have minima displaced along the vibrational coordinate by the amount ΔQ_v.[44,45] The parameter S is usually referred to as the Huang−Rhys factor and is given by

$$S = \frac{\mu\omega_v \Delta Q_v^{\,2}}{2\hbar} \qquad (3)$$

where μ is the reduced mass of the vibrational mode.[46] In the above equations the mode index has been omitted. The parameter S is thus related to the change in geometry between the ground and the excited state of the molecule.

TABLE 2: Experimental One- and Two-Photon Spectroscopic Parameters, Fluorescence Lifetimes, and Electrochemical Potentials for Molecules 1−6

	1	**2**	**3**	**4**	**5**[a]	**6**[a]
$\lambda_{abs}^{(1)}$ (nm)[b]	490	475	438	440	410	411
ϵ (M^{-1} cm^{-1})[b]	6.6×10^4	6.6×10^4	5.4×10^4	5.0×10^4	7.4×10^4	6.3×10^4
$\lambda_{fl}^{(1)}$ (nm)[c]	536	528	504	510	455	457
η[d]	0.69	0.87	0.003	0.015	0.88	0.93
τ (ns)[d]	1.30	1.46	<0.015	0.074		
$E_{M^+/M}$ (mV)[e]	+260	+535	+390	+630	+90	+350
$\lambda_{abs}^{(2)}$ (nm)[f]	830	830	790	825	730	745
	(830)	(840)	(800)	(825)	(725)	
δ (GM)[f]	1750	1640	890	730	995	805
	(1710)	(1890)	(860)	(690)	(635)	
k_r (10^8 s^{-1})[g]	5.30	5.97	>2	2.04		
k_{nr} (10^8 s^{-1})[g]	2.38	0.892	> 660	134		

[a] From refs 8 and 9. [b] One-photon absorption maximum ($\lambda_{abs}^{(1)}$) and peak molar extinction coefficient (ϵ). [c] One-photon fluorescence maximum. [d] Fluorescence quantum yield (η) and fluorescence lifetime (τ). The uncertainty in η is 5% for **1** and **2**, and about 10% for **3** and **4**. The uncertainty in τ is less than 1% for **1** and **2** and is about 10% for **4**. [e] Electrochemical potential vs FcH/Fc in THF. [f] Maximum of the two-photon fluorescence excitation spectrum ($\lambda_{abs}^{(2)}$) and peak two-photon cross section (δ); 1 GM $\equiv 1 \times 10^{-50}$ cm^4 s photon^{-1} molecule^{-1}. The uncertainty in δ is ±15%. The values in parentheses refer to the femtosecond-pulse measurements, the other to nanosecond-pulse measurements. The reference compound used was fluorescein. [g] Rate constants for radiative (k_r) and nonradiative (k_{nr}) decay (eq 5).

In the room temperature absorption spectra of many conjugated molecules in solution, often only one or two progressions of vibronic components can be identified.[47] We included only one vibrational mode in our analysis of the spectra of **1**−**6**. The following equation was used for the fitting of the experimental absorption spectra:

$$A(E) = \sum_{v''=0}^{m} A_0 \frac{S^{v''}}{v''!} \exp\left(-\frac{(E - E_{0-0} - v''E_{vib})^2}{\Gamma^2}\right) \quad (4)$$

In eq 4, the vibronic components are described by Gaussian line shapes characterized by the same width, Γ, equally spaced by the amount $E_{vib} = \hbar\omega_v$, and with intensities relative to the $v'' = 0$ band given by the square of eq 2. E_{0-0} corresponds to the energy of the transition between the $v' = 0$ vibronic level of state g and the $v'' = 0$ vibronic level of state e. $A(E)$ is the absorbance at energy E, and A_0 is the peak absorbance of the 0−0 vibronic component of the progression. For the fitting, we used the lowest four components of the progression ($m = 3$) and included the experimental points up to energies just above the absorption maximum, to avoid the influence of the higher energy shoulder (see below). The fitting results for the absorption spectra of molecules **1**−**6** are reported in Table 3 and in Figure 4A. The fitting curves reproduce well the features of the absorption spectra of molecules **1**−**4** in the region around the absorption maximum and at lower energies, and those of molecules **5** and **6** over the whole absorption band. As mentioned above, eq 2 is valid if the frequencies of the main vibrational mode in the ground and excited states are the same. This is not true in general, but the results of the fittings performed on both the absorption and fluorescence spectra of molecules **1**−**6** indicate that the change in vibrational frequencies is small in this case (see below), within the resolution of solution-phase spectra. Moreover, the change in the value of the overlap integral when distinct vibrational frequencies for the ground and excited states are introduced is relatively small for the 0−0 and 0−1 components, which contain most of the experimental points used for the fittings.

TABLE 3: Results of the Franck−Condon Analysis for the One-Photon Absorption and Fluorescence Spectra for Molecules 1−6, and Experimental Determination of the Transition Dipole Moments

	1	**2**	**3**	**4**	**5**	**6**
One-Photon Absorption Data						
E_{0-0} (eV)[a]	2.500	2.559	2.640	2.641	2.857	2.868
ω_v (cm^{-1})[b]	1315	1327	1227	1178	1327	1325
Γ (eV)[c]	0.1111	0.1162	0.1232	0.1215	0.1052	0.1108
S[d]	0.886	0.948	1.725	1.600	1.406	1.359
area of band e (eV)[e]	0.4206	0.4435	0.5294	0.4929	0.4950	0.4936
area of band f (eV)[e]	0.1464	0.0854	0.1909	0.1689	0.0123	0.0269
E_{gf} (eV)[f]	3.061	3.171	3.246	3.212		
M_{ge} (D)[g]	10.0	10.1	9.64	8.98	10.5	9.71
M_{gf} (D)[g]	5.38	3.80	5.40	4.91		
Fluorescence Emission Data						
E_{0-0} (eV)[a]	2.327	2.356	2.475	2.437	2.724	2.714
ω_v (cm^{-1})[b]	1259	1310	1408	1373	1374	1388
Γ (eV)[c]	0.0982	0.1023	0.1032	0.1051	0.0875	0.0888
S[d]	0.636	0.630	0.714	0.646	0.874	0.818
Two-Photon Absorption Data						
$M_{ee'}$ (D)[h]	15.1	15.5	12.9	13.6	12.2	12.1
$E_{ge} - {}^1/_2E_{ge'}$ (eV)[i]	1.04	1.12	1.26	1.30	1.33	1.37
$E_{gf} - {}^1/_2E_{ge'}$ (eV)[i]	1.57	1.68	1.68	1.71		

[a] Energy of the peak of the 0−0 vibronic component. [b] Vibrational frequency. [c] Width of the Gaussian vibronic components. [d] Huang−Rhys factor. [e] Area of the lower energy band (g → e), calculated as the sum of the areas of the six lowest components of the progression obtained from the F−C analysis, and of the higher energy band (residual band, g → f) in the absorption spectra. The areas reported are calculated from the spectra in Figure 4A where the experimental absorption maxima have been normalized to one. The integrated extinction coefficients, $\int\epsilon(E)\,dE$, are obtained by multiplying these areas by the peak molar extinction coefficients. [f] Energy at the maximum of the residual band (energy of the transition g → f). [g] Transition dipole moments (in Debye, D) for the transitions g → e and g → f. [h] Transition dipole moments for the transition e → e′ (eq 6) assuming a negligible contribution to δ from state f (see text). [i] Energy detuning terms.

The F−C analysis shows that the 0−0 vibronic transition is the strongest component in the case of **1** ($S = 0.89$). The same is true for **2**, but the S factor is slightly larger in this case ($S = 0.95$), such that the absorption maximum is at higher energy than E_{0-0}. The analysis indicates that the change in geometry between the ground state and the excited state is larger for compound **2** than compound **1**. The analysis also shows that E_{0-0} is actually very similar for the two molecules, in contrast to the apparent shift in $\lambda_{abs}^{(1)}$.

The absorption bands for **3** and **4** are broader than for **1** and **2**, as a consequence of larger values of S for **3** and **4** ($1.5 < S < 2$), leading to a distribution of the absorption intensity over a larger number of vibronic components. Moreover, each vibronic band is wider (larger Γ values) for **3** and **4** than for **1** and **2**, probably due to the larger degree of conformational disorder and resulting wider distribution of torsion angles for the phenylene rings in the ground state for the vinyl-substituted molecules. This finding is consistent with a shallower potential energy surface for the vinyl-substituted molecules than for the phenylene-substituted molecules.[48] At ≈3.1 eV, **3** and **4** exhibit a clear shoulder in the absorption spectrum. As this shoulder is located at 0.4−0.5 eV higher energy than E_{0-0}, it is unlikely to be a vibronic component of the main band, but rather could be due to a transition to a higher energy excited state. Similarly, a seemingly weaker higher energy shoulder is visible in the absorption spectra of **1** and **2** but is not seen in **5** and **6**. If the bands obtained from the F−C analysis are subtracted from the experimental absorption spectra, a residual band can clearly be seen (Figure 4A), with a maximum at 3.1−3.2 eV for **1**−**4** (see Table 3). The band shape analysis shows that the relative

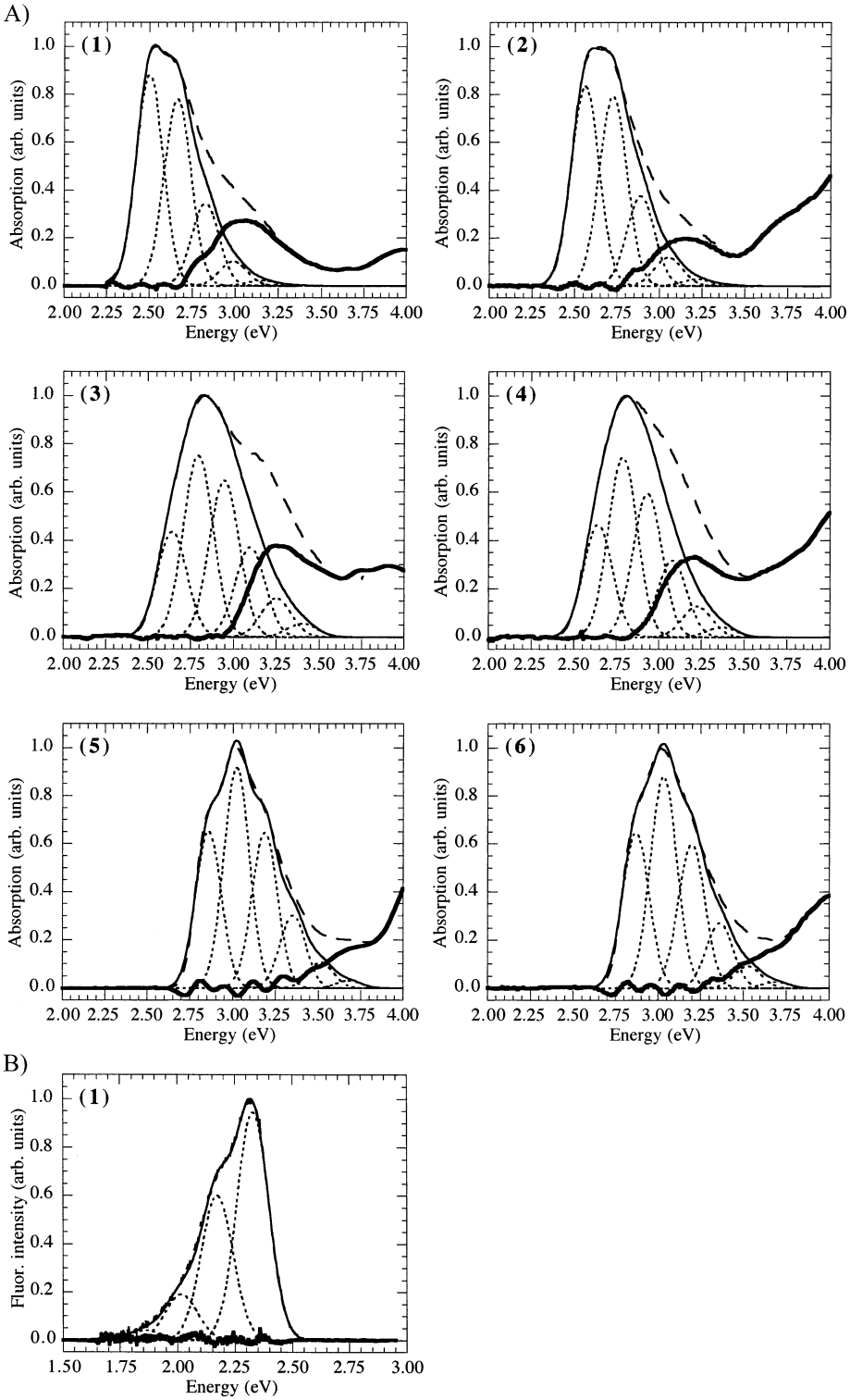

Figure 4. Franck−Condon band shape analysis of (A) the absorption spectra of compounds **1**−**6**; (B) the fluorescence spectrum of **1**: (dashed line) experimental spectrum; (dotted lines) vibronic components of the main absorption or fluorescence band; (thin solid line) sum of the first six vibronic components of the main band; (thick solid line) difference between the experimental spectrum and the fitting results (residual).

intensities of the high- to the low-energy bands are comparable for **1**−**4**, ranging from 0.19 to 0.36, with no clear dependence on the substitution pattern of the conjugated chain. In the case of **5** and **6**, instead, the fitted F−C band shape accounts for the whole absorption band and no contribution from a higher lying state is visible. It should be noted that the positions of the residual bands in the one-photon spectra are very close in energy to the peaks of the two-photon spectra for **1**−**4**. These higher energy bands in the one-photon spectra may be due to a transition to the lowest allowed two-photon state which has gained intensity by vibronic coupling or a symmetry breaking distortion, or it may be due to an accidental degeneracy of this two-photon state and an allowed, but weaker, one-photon state. In fact, such a weakly allowed one-photon state is obtained from quantum chemical calculations on these molecules. In the following discussions, the higher lying excited state responsible for the residual band will be indicated as state f. The presence of a higher energy shoulder or peak (3.6−3.8 eV) in the

absorption spectrum has been reported for other substituted bisstyrylbenzenes,[49−52] but the origin of this band has not been clearly identified.

Band Strength of Low-Energy Electronic Transitions. The peak extinction coefficients of the low-energy bands for **1** and **2** are similar to those for the unsubstituted molecules **5** and **6** and are larger than the values for **3** and **4**. However, the transition dipole moments M_{ge} calculated from the integrated absorption strengths[43,53] of the lower energy band are similar for the molecules with and without cyano substitution (M_{ge} = 9.0−10.5 D for molecules **1**−**6**). This result is in agreement with what was reported by Rumi et al.[9] for D−π−D molecules, where it was found that the magnitude of M_{ge} is primarily determined by the conjugation length and type of π-bridge, rather than the donor substitution of the π-system. The present experimental results indicate that M_{ge} does not strongly depend on the position of the acceptor substitution. The quantum chemical calculations (section vi) support this finding and also show that, for a given molecule, M_{ge} is only weakly dependent on the torsional configuration of the π-backbone over the range of P_L-P_C angles of ≈0−72°. The transition dipole moments M_{gf} are in the range 3.8−5.4 D, about a factor of 2 smaller than the M_{ge}'s. The values of M_{gf} are largest for the D−A−D molecules with di-*n*-butylamino donor groups (**1** and **3**).

Fluorescence Spectroscopy. Similar to what is observed for the absorption spectra, the fluorescence spectra of compounds **1** and **2** are red-shifted with respect to **3** and **4**. The fluorescence bands are similar in shape for molecules **1**−**4** and show some vibronic structure. An F−C analysis similar to the one described above for the absorption spectra was carried out for the fluorescence spectra of **1**−**6**. In this case, eq 4 was modified as follows: $F(E)$ and F_0, the fluorescence intensity at energy E and at the peak of the 0−0 vibronic component, were introduced in place of the corresponding absorbances, υ'' was replaced by υ', and the sign in front of $\upsilon' E_{vib}$ was changed. The modified eq 4 fits reasonably well the experimental fluorescence spectra (see Figure 4B for a representative example) and the fitting parameters are included in Table 3. All the spectra are 0−0 peaked ($S < 1$) and the vibronic components have slightly narrower bandwidths than for the absorption (smaller Γ). The narrower bandwidths indicate that there is a steeper potential surface for torsional motions in the excited state than in the ground state. Semiempirical calculations (at the AM1 level) with single and double configuration interactions show that this is the case for stilbene.[54] This is also consistent with the stiffening of the calculated ring-torsion normal modes (librations) in the excited state with respect to the ground state for PPV oligomers containing two to five rings.[55] The results of the fitting show that the Huang−Rhys factors for the fluorescence spectra are much smaller than for the absorption spectra, as has been observed for other substituted distyrylbenzenes[51] and for PPV oligomers of various conjugation lengths.[46,48] The same pattern has also been reproduced by a semiempirical quantum chemical approach in which the contributions of multiple vibrational modes were taken into account in the calculation of the intensity distribution in absorption and emission transitions of PPV oligomers.[54]

Several recent papers[48,49,51] suggest that the first excited state of some substituted PPV oligomers is more planar than the ground state. The primary evidence to support this conclusion is that the vibronic structure is more pronounced in the fluorescence spectrum than in the absorption spectrum. For the molecules studied here (**1**−**4**), the fluorescence spectra are all very similar in shape, which is indicative of similar geometries for the relaxed excited state. The presence of donor and acceptor groups on the π-backbone could lead to excited states with highly delocalized charge distributions, which would facilitate the planarization of the molecule upon excitation (due to stronger quinoid contributions to the relaxed excited-state geometry), with respect to an unsubstituted conjugated system. As discussed above, the absorption spectra are broader than the fluorescence spectra and are broadest for the vinyl-substituted molecules, suggesting the fact that the ground-state torsional potential energy surface is relatively flat around the minimum for these molecules. Inspection of Figure 3 shows that the Stokes' shift (the energy spacing between $\lambda_{abs}^{(1)}$ and $\lambda_{fl}^{(1)}$) is larger for molecules **3** (2990 cm^{-1}) and **4** (3120 cm^{-1}), which have the cyano group substituted on the double bond, than for molecules **1** (1750 cm^{-1}) and **2** (2110 cm^{-1}), with the cyano group substituted on the central phenylene ring. This suggests that for molecules **3** and **4** there is a larger change in geometry along the coordinate corresponding to the dominant high-frequency vibrational mode in going from the ground to the excited state than there is for **1** and **2**, as would be the case if the excited state were planar or near planar. Moreover, the energy differences between the E_{0-0}'s from the fits of the absorption and fluorescence spectra are larger in the molecules with diphenylamino end groups than for those with di-*n*-butylamino end groups, when the comparison is made between molecules with the same acceptor substitution. For example, the energy differences are 0.173 and 0.203 eV for molecules **1** and **2**, respectively. This indicates that the solvent and low-frequency vibrational reorganization energy is larger for the molecules containing the diphenylamino groups, perhaps due to the rotation of the phenyl ring around the C−N bond.

For all molecules, the vibronic spacings, ω_υ, in the absorption and fluorescence spectra are comparable (1200−1400 cm^{-1}). In the Raman spectrum of PPV oligomers, two strong, totally symmetric vibrational modes are observed around 1600 and 1200 cm^{-1}.[56] In the molecules studied here, the vibronic spacings range from being intermediate between the two modes of the PPV oligomers to being close to the lower frequency mode. Similar spacings have been observed in absorption and fluorescence spectra of other PPV derivatives containing up to 5 phenylene rings[46,48] and methoxy-substituted distyrylbenzenes.[51] The closeness of the ω_υ values in the absorption and fluorescence spectra provides justification for the utilization of the overlap integral in eq 2, which assumes that ground and excited states are characterized by the same vibrational frequency.

Fluorescence Quantum Yields and Lifetimes. The position of the cyano substituents has a pronounced effect on the fluorescence quantum yield, η, of these chromophores. Specifically, molecules **1** and **2**, as well as **5** and **6**, are highly fluorescent ($\eta \geq 0.7$), whereas η is drastically reduced for cyano substitution on the vinylene double bond (η = 0.003 for **3**, 0.015 for **4**). The fluorescence lifetimes, τ, of molecules **1** and **2** are slightly longer than 1 ns and are similar to those for D−π−D distyrylbenzenes (measured in acetonitrile).[9] In contrast, the fluorescence lifetimes for **3** and **4** are reduced to less than 100 ps. The rate constants for radiative (k_r) and nonradiative (k_{nr}) decays can be estimated from the fluorescence quantum yields and lifetimes[57] using eq 5 and are included in Table 2:

$$\eta = \frac{k_r}{k_r + k_{nr}} \quad \text{and} \quad \tau = (k_r + k_{nr})^{-1} \tag{5}$$

Whereas the values of k_r are similar for all the molecules, k_{nr}

increases by 2 orders of magnitude for molecules **3** and **4** relative to **1** and **2**. The large deviation from planarity in the vinyl-substituted molecules may explain the low quantum yield and large k_{nr} of molecules **3** and **4** because the torsional vibrations of the molecule offer fast nonradiative decay pathways.[49,58]

Similar results for η, τ, and k_{nr} have been reported for other classes of phenylene vinylene oligomers in which cyano groups are substituted on the vinyl bonds of the π-backbone at the carbon adjacent to the central phenylene.[49,50,58,59] When the substitution is on the vinyl carbon closer to the extremity of the molecule, the fluorescence is not suppressed as strongly and the lifetime is more similar to that of the unsubstituted molecules, if no other substituents are present on the outer rings.

Two-Photon Spectroscopy. The two-photon spectra (Figure 3) of the different molecules are also affected by the presence and the position of the cyano substitution on the π-backbone. As in the one-photon spectra, the addition of acceptor groups to the molecule shifts the two-photon peak to the red, with the molecules having the substitution on the phenylene, **1** and **2**, showing the largest shift relative to the unsubstituted **5** and **6**. All of the two-photon bands are somewhat narrow, with full widths at half-maximum in the range 0.27−0.38 eV. A discussion of the two-photon cross-sections will be addressed later in section v.

(iv) State Ordering. As previously observed for D−π−D compounds,[9] the D−A−D molecules with dibutylamino groups have higher energy HOMO levels than those with diphenylamino groups. For example, the electrode potential of the half-reaction M^+ to M ($E_{M^+/M}$) is about 240 mV larger for molecule **4** than for **3**. The presence of cyano acceptor groups reduces the donating ability of the molecules (see Table 2) and results in a lowering of the energy of the HOMO level with respect to D−π−D chromophores. For molecules **1** and **3**, which have different positions of acceptor substitution, the $E_{M^+/M}$ potentials are +260 and +390 mV, respectively, whereas the value for the unsubstituted **5** is +90 mV. A similar trend is observed for the diphenylamino-substituted molecules **2**, **4**, and **6**. This indicates that the compounds with the cyano substitution on the vinyl bond are weaker donors than the molecules with the cyano substitution on the central phenylene. This is different than what was reported by Liu et al.,[60] for chromophores analogous to **1** and **3** (or **2** and **4**), but with terminal *tert*-butyl groups instead of terminal alkyl- or arylamino donor groups. In their studies, it was found that the compound with cyano groups on the vinyls and that with substitution on the central phenylene had only slightly different HOMO (and LUMO) energies. This can be understood as a result of a near balance of the effects of the distortion of the π-backbone and the influence of the electron acceptors on the HOMO energies. However, in the molecules studied here, the HOMO energy is strongly influenced by the presence of the terminal donor and its coupling to the acceptor. As a consequence, when the acceptor is well conjugated and close to the donor group, the donor strength is diminished (the HOMO level would be lowered), as in the case of **3** relative to **1** (or **4** relative to **2**).

Figure 5 displays the one- and two-photon (e′) state energies of molecules **1**−**6** relative to the ground state. It is apparent that the spacing between the one- and two-photon absorption maxima is much smaller in **4** (0.19 eV) than in all the other molecules studied here (0.27−0.46 eV). This can be understood as primarily due to two effects. One is the shift of the e state of **4** to higher energy relative to **2**, which can be related to a decrease in the effective conjugation length due to the nonplanarity of the π-backbone. The other effect is the shift to lower

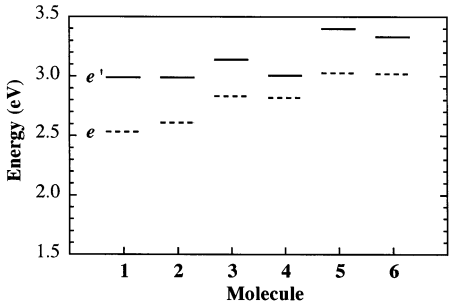

Figure 5. Energy of the first (e) and two-photon excited (e′) states. The energies of states e and e′ relative to the ground state (g), E_{ge} (dashed lines) and $E_{ge'}$ (solid lines), are given by $hc/\lambda_{abs}^{(1)}$ and $2hc/\lambda_{abs}^{(2)}$, respectively.

energy of the e′ level of **4** with respect to **3** as a result of the presence of phenyl groups on the amino donors (as has been discussed previously[9]). Quantum chemical calculations, which will be discussed below in section vi, show similar trends and support this analysis.

(v) Two-Photon Cross Sections. All the molecules studied here have been found to be relatively strong two-photon absorbers. We have obtained results[61] for the two-photon excitation maximum, $\lambda_{abs}^{(2)}$, and δ using both nanosecond and femtosecond pulses and found them to be in good agreement with each other. The magnitude of δ for the vinylene-substituted molecules, **3** and **4** (δ = 890 and 730 GM, respectively; 1 GM $\equiv 1 \times 10^{-50}$ cm^4 s photon^{-1} molecule^{-1}), is substantially lower than for the phenylene-substituted molecules (δ = 1750 and 1640 GM for **1** and **2**, respectively), and is similar to the value for the unsubstituted molecules (δ = 995 and 805 GM for **5** and **6**, respectively). This result indicates that the position of the acceptor substitution in D−A−D molecules and the planarity of the π-system are critical and the mere presence of acceptor groups is not always effective in enhancing the molecular two-photon response. These results can be understood in terms of the distance between the donor and acceptor groups and, for the vinyl-substituted molecules, the reduced conjugation due to the nonplanarity of the π-backbone.

In a simplified description for linear quadrupolar molecules that includes three electronic states, g, e, and e′, it can be shown that the peak two-photon cross section is given by[9,62]

$$\delta \approx \frac{16\pi^2\hbar\omega^2 L^4}{5n^2c^2} \frac{M_{ge}{}^2 M_{ee'}{}^2}{(E_{ge} - \hbar\omega)^2 \Gamma_{ge'}} \qquad (6)$$

where ω is the excitation frequency at the peak of the two-photon absorption band ($\hbar\omega = {}^1/_2 E_{ge'}$), n is the refractive index of the solvent, c is the speed of light, L is the local field factor, and $\Gamma_{ge'}$ is the damping factor. The energy difference in the denominator of eq 6 ($E_{ge} - \hbar\omega$) is usually called the detuning term. The transition moments M_{ge} were obtained from the area of the low-energy band in the absorption spectrum. The transition moments $M_{ee'}$ were obtained using eq 9 of ref 9 and are reported in Table 3 (a value of 0.1 eV was assumed for the damping factor in all cases). Unlike M_{ge}, which does not vary significantly with cyano substitution, $M_{ee'}$ is largest for molecules **1** and **2** (≈15 D). As in the trends for δ, $M_{ee'}$ values for **3** and **4** are similar to those for **5** and **6** (12−13 D). $M_{ee'}$ is thus the molecular parameter that is most strongly affected by the acceptor substitution pattern in D−A−D conjugated systems, as it was by the presence of donor end groups in D−π−D molecules.[8,9]

TABLE 4: Spectroscopic Parameters Determined by Quantum Chemical Calculations on Model Compounds 1c and 3c[a]

molecule	E_{ge} (eV)	M_{ge} (D)	$^1/_2E_{ge'}$ (eV)	δ (GM)	$M_{ee'}$ (D)
1c[b]	3.26	12.4	1.98	947	11.9
3c[b]	3.28	12.7	e_i': 1.90	e_i': 174	e_i': 4.5
			e_{ii}': 2.06	e_{ii}': 624	e_{ii}': 8.6
5c[b,c]	3.42	13.3	2.09	682	9.1
1c′[d]	3.42	12.4	1.96	251	7.3
3c′[d]	3.61	11.8	e_i': 1.94	99	6.0
			e_{ii}': no resonance		

[a] The symbols have the same meanings as in Tables 2 and 3 and Figure 5. See text for definition of states e_i' and e_{ii}'. [b] Planar conformation. [c] Data for molecule **5c** are taken from ref 8. [d] Using the conformation from the crystal structures of **2** in the case of **1c′** and **4** in the case of **3c′**.

As discussed in section iii, the two-photon state e′ is close in energy to state f identified in the absorption spectra of **1**−**4**. If this were a state distinct from e′, it could act as another intermediate state for the two-photon absorption process, in a sum-over-states description. In this case, the three-level description given above is not appropriate and at least four states should be considered. However, even assuming $M_{fe'} \approx M_{ee'}$, the contribution to δ from state f would be almost an order of magnitude smaller than that from state e (and thus be comparable to the uncertainty in the measurements), because $M_{gf} \approx {}^1/_2M_{ge}$ and the energy detuning term is much larger for state f than e (1.68 and 1.26 eV, respectively, for molecule **3**, for example). The values of $M_{ee'}$ reported in Table 3 were obtained by neglecting the contribution from state f.

(vi) Quantum Chemical Calculations. To better understand the effect of the ground state conformation on the energy and strengths of the electronic transitions, quantum chemical calculations have been performed on the model compounds **1c** and **3c** (see Figure 1), in which planar geometries have been imposed, and **1c′** and **3c′**, in which the geometries obtained from the crystallographic data of **2** and **4**, respectively, were used.[63] For the reasons discussed previously,[8] all of the calculated excited-state energies appear to be larger than the experimental values. As a result, this approach leads to lower calculated values for δ; however, it provides reasonable trends for a consistent series of molecules. The results reported here are for vertical transitions; thus no change in geometry between the ground state and excited state has been explicitly included. For **3c**, two closely spaced two-photon transitions are obtained (Table 4). The final state at lower energy, e_i', can be described as a charge transfer between the amino donor and the cyano acceptor groups, whereas the higher energy state, e_{ii}', can be described as a charge transfer from the amino donors to the central phenylene ring. State e_{ii}' is similar in energy and character to the two-photon state of the unsubstituted molecule **5c**. For the planar configuration, the overall two-photon cross section for the two closely lying states of **3c** is intermediate to those for **5c** and **1c**. This trend in δ is likely due to the shorter donor−acceptor distance over which intramolecular charge transfer can take place in **3c** compared to **1c**.

When the distorted conformations are considered (**1c′** and **3c′**), the position of the one-photon state is blue-shifted and the value of δ is substantially reduced compared to **1c** and **3c**, respectively, but the energy of the two-photon state is only slightly affected. This shows that the planarity of the molecular configuration is very important in determining the magnitude of δ. It should be noted that for molecule **3c′**, state e_{ii}' is no longer two-photon active in the nonplanar conformation and state e_i' is only weakly affected by the distortion, as it involves mainly the interaction between the donor and acceptor groups on each half of the molecule. The δ value for **3c′** is much smaller than for **1c′**, consistent with the experimental observations on **1** and **3** (or **2** and **4**). However, the calculated δ values for **1c′** and **3c′** are small compared to those for **5c**, whereas **1** and **3** exhibit experimental δ values that are larger by a factor of 2 (for molecule **1**) or comparable (in the case of **3**) to **5**. This could be explained if the range of torsional motion for the molecules in solution is sufficiently large that conformations corresponding to large δ values are sampled.

The agreement between the calculated and experimental M_{ge} values is reasonably good, whereas the calculated $M_{ee'}$'s are substantially lower than the experimental ones, corresponding to the underestimation of δ. The calculated values for M_{ge} do not depend significantly on the conformation and are very similar for all cases. This substantiates the experimental finding that the values of M_{ge} are mostly determined by the type of π-bridge and less so by the position of the substitution or by the conformation. In contrast, $M_{ee'}$ is generally reduced upon distortion of the π-backbone and $M_{ee'}$ for vinyl-substituted molecules is smaller than for the phenylene-substituted molecules.

Conclusions

We have shown that in D−A−D type molecules, the position of the acceptor substitution on the conjugated bridge can greatly affect the one- and two-photon properties of the chromophores. From the absorption and fluorescence spectroscopy on the molecules studied here, we conclude that (1) the molecules that are highly distorted in the ground state undergo a larger change in geometry upon excitation than the more planar ones, (2) all the molecules examined undergo a relatively small change in geometry upon emission and exhibit rather sharp features in the fluorescence spectra, and (3) these results are consistent with a relaxation in the lowest excited state to a somewhat planar geometry which is similar for all the molecules and with this relaxed state having a steeper potential for torsional motion of the rings than does the ground state. These conclusions are consistent with what has been described for related PPV oligomers and derivatives. Molecules with a large torsional distortion in the ground state undergo fast nonradiative decay and show small fluorescence quantum yields. Further studies on the relaxation processes and dynamics are needed to clarify the nature of the relaxed excited state. For distyrylbenzenes with terminal amino donor groups, the two-photon cross section is larger by a factor of 2 when cyano acceptor groups are substituted on the central phenylene than when the substitution is on the vinyl groups. These results have been rationalized in terms of the difference in the distance between the donor and acceptor groups and the degree of distortion from planarity in the ground state, and their effects on intramolecular charge transfer. Clearly, the interplay of the substituent position, electronic coupling, and torsional conformation is an important consideration in the design of fluorescent chromophores with large two-photon cross sections.

Acknowledgment. This material is based upon work supported by the National Science Foundation under Grant No. CHE-0107105 and CHE-0078819, the Office for Naval Research (Grant No. N00014-95-1-1319 and N00014-01-1-0615), the Air Force Office of Scientific Research (Grant No. F49620-02-1-0358), and the AFOSR Defense University Research Instrumentation Program (Grant No. F49620-99-1-0161), which are gratefully acknowledged. The work in Mons has been partly

supported by the Belgian Federal Government "Inter-University Attraction Pole 5/3" and FNRS. We thank Stephen Barlow, David Carrig, Stephen M. Kuebler, and Wim Wenseleers for technical assistance.

Supporting Information Available: X-ray crystal structures of compounds **2** and **4**. This material is available free of charge via the Internet at http://pubs.acs.org.

References and Notes

(1) Denk, W.; Strickler, J. H.; Webb, W. W. *Science* **1990**, *248*, 73−76.

(2) Fisher, W. G.; Partridge, W. P., Jr.; Dees, C.; Wachter, E. A. *Photochem. Photobiol.* **1997**, *66*, 141−155.

(3) Spangler, C. W. *J. Mater. Chem.* **1999**, *9*, 2013−2020.

(4) Wu, E. S.; Strickler, J. H.; Harrell, W. R.; Webb, W. W. *Proc. SPIE* **1992**, *1674*, 776−782.

(5) Maruo, S.; Nakamura, O.; Kawata, S. *Opt. Lett.* **1997**, *22*, 132−134.

(6) Cumpston, B. H.; Ananthavel, S. P.; Barlow, S.; Dyer, D. L.; Ehrlich, J. E.; Erskine, L. L.; Heikal, A. A.; Kuebler, S. M.; Lee, I.-Y. S.; McCord-Maughon, D.; Qin, J.; Röckel, H.; Rumi, M.; Wu, X.-L.; Marder, S. R.; Perry, J. W. *Nature* **1999**, *398*, 51−54.

(7) Zhou, W.; Kuebler, S. M.; Braun, K. L.; Yu, T.; Cammack, J. K.; Ober, C. K.; Perry, J. W.; Marder, S. R. *Science* **2002**, *296*, 1106−1109.

(8) Albota, M.; Beljonne, D.; Brédas, J.-L.; Ehrlich, J. E.; Fu, J.-Y.; Heikal, A. A.; Hess, S. E.; Kogej, T.; Levin, M. D.; Marder, S. R.; McCord-Maughon, D.; Perry, J. W.; Röckel, H.; Rumi, M.; Subramaniam, G.; Webb, W. W.; Wu, X.-L.; Xu, C. *Science* **1998**, *281*, 1653−1656.

(9) Rumi, M.; Ehrlich, J. E.; Heikal, A. A.; Perry, J. W.; Barlow, S.; Hu, Z.; McCord-Maughon, D.; Parker, T. C.; Röckel, H.; Thayumanavan, S.; Marder, S. R.; Beljonne, D.; Brédas, J.-L. *J. Am. Chem. Soc.* **2000**, *122*, 9500−9510.

(10) Reinhardt, B. A.; Brott, L. L.; Clarson, S. J.; Dillard, A. G.; Bhatt, J. C.; Kannan, R.; Yuan, L.; He, G. S.; Prasad, P. N. *Chem. Mater.* **1998**, *10*, 1863−1874.

(11) Ventelon, L.; Moreaux, L.; Mertz, J.; Blanchard-Desce, M. *Chem. Commun.* **1999**, 2055−2056.

(12) Zojer, E.; Beljonne, D.; Kogej, T.; Vogel, H.; Marder, S. R.; Perry, J. W.; Brédas, J. L. *J. Chem. Phys.* **2002**, *116*, 3646−3658.

(13) Kotler, Z.; Segal, J.; Sigalov, M.; Ben-Asuly, A.; Khodorkovsky, V. *Synth. Met.* **2000**, *115*, 269−273.

(14) Morel, Y.; Irimia, A.; Najechalski, P.; Kervella, Y.; Stephan, O.; Baldeck, P. L.; Andraud, C. *J. Chem. Phys.* **2001**, *114*, 5391−5396.

(15) Najechalski, P.; Morel, Y.; Stéphan, O.; Baldeck, P. L. *Chem. Phys. Lett.* **2001**, *343*, 44−48.

(16) Cho, B. R.; Son, K. H.; Lee, S. H.; Song, Y.-S.; Lee, Y.-K.; Jeon, S.-J.; Choi, J. H.; Lee, H.; Cho, M. *J. Am. Chem. Soc.* **2001**, *123*, 10039−10045.

(17) Beljonne, D.; Wenseleers, W.; Zojer, E.; Shuai, Z.; Vogel, H.; Pond, S. J. K.; Perry, J. W.; Marder, S. R.; Brédas, J. L. *Adv. Funct. Mater.* **2002**, *12*, 631−641.

(18) Chung, S.-J.; Kim, K.-S.; Lin, T.-C.; He, G. S.; Swiatkiewicz, J.; Prasad, P. N. *J. Phys. Chem. B* **1999**, *103*, 10741−10745.

(19) Drobizhev, M.; Karotki, A.; Rebane, A.; Spangler, C. W. *Opt. Lett.* **2001**, *26*, 1081−1083.

(20) Chen, D.; Winokur, M. J.; Masse, M. A.; Karazs, F. E. *Polymer* **1992**, *33*, 3116−3122.

(21) Mao, G.; Fischer, J. E.; Karasz, F. E.; Winokur, M. J. *J. Chem. Phys.* **1993**, *98*, 712−716.

(22) van Hutten, P. F.; Wildeman, J.; Meetsma, A.; Hadziioannou, G. *J. Am. Chem. Soc.* **1999**, *121*, 5910−5918.

(23) Hohloch, M.; Maichle-Mössmer, C.; Hanack, M. *Chem. Mater.* **1998**, *10*, 1327−1332.

(24) Bartholomew, G. P.; Bazan, G. C.; Bu, X.; Lachicotte, R. J. *Chem. Mater.* **2000**, *12*, 1422−1430.

(25) Gill, R. E.; Hilberer, A.; van Hutten, P. F.; Berentschot, G.; Werts, M. P. L.; Meetsma, A.; Wittmann, J.-C.; Hadziioannou, G. *Synth. Met.* **1997**, *84*, 637−638.

(26) Fahlman, M.; Brédas, J. L. *Synth. Met.* **1996**, *78*, 39−46.

(27) Pati, S. K.; Marks, T. J.; Ratner, M. A. *J. Am. Chem. Soc.* **2001**, *123*, 7287−7291.

(28) Poulsen, T. D.; Frederiksen, P. K.; Jørgensen, M.; Mikkelsen, K. V.; Ogilby, P. R. *J. Phys. Chem. A* **2001**, *105*, 11488−11495.

(29) Wenseleers, W.; Stellacci, F.; Meyer-Friedrichsen, T.; Mangel, T.; Bauer, C. A.; Pond, S. J. K.; Marder, S. R.; Perry, J. W. *J. Phys. Chem. B* **2002**, *106*, 6853−6863.

(30) Xiao, Y.; Yu, W.-L.; Chua, S.-J.; Huang, W. *Chem. Eur. J.* **2000**, *6*, 1318−1321.

(31) Pinto, M. R.; Hu, B.; Karasz, F. E.; Akcelrud, L. *Polymer* **2000**, *41*, 2603−2611.

(32) Baker, T. N., III; Doherty, W. P., Jr.; Kelley, W. S.; Newmeyer, W.; Rogers, J. E., Jr.; Spalding, R. E.; Walter, R. I. *J. Org. Chem.* **1965**, *30*, 3714−3718.

(33) Sheldrick, G. M. *Acta Crystallogr. A* **1990**, *46*, 467−473.

(34) Berlman, I. B. *Handbook of Fluorescence Spectra of Aromatic Molecules*, 2nd ed.; Academic Press: New York, 1971.

(35) O'Connor, D. V.; Phillips, D. *Time-correlated Single Photon Counting*; Academic Press: London, 1984.

(36) Khundkar, L. R.; Perry, J. W.; Hanson, J. E.; Dervan, P. B. *J. Am. Chem. Soc.* **1994**, *116*, 9700−9709.

(37) Xu, C.; Webb, W. W. *J. Opt. Soc. Am. B* **1996**, *13*, 481−491.

(38) Fisher, W. G.; Wachter, E. A.; Lytle, F. E.; Armas, M.; Seaton, C. *Appl. Spectrosc.* **1998**, *52*, 536−545.

(39) Dewar, M. J. S.; Zoebisch, E. G.; Healy, E. F.; Stewart, J. J. P. *J. Am. Chem. Soc.* **1985**, *107*, 3902−3909.

(40) Ridley, J.; Zerner, M. *Theor. Chim. Acta* **1973**, *32*, 111−134.

(41) Orr, B. J.; Ward, J. F. *Mol. Phys.* **1971**, *20*, 513−526.

(42) Ehrlich, J. E.; Wu, X. L.; Lee, I.-Y. S.; Hu, Z.-Y.; Röckel, H.; Marder, S. R.; Perry, J. W. *Opt. Lett.* **1997**, *22*, 1843−1845.

(43) Herzberg, G. *Molecular Spectra and Molecular Structure. I. Spectra of Diatomic Molecules*, 2nd ed.; Van Nostrand Reinhold Co.: New York, 1950.

(44) Coon, J. B.; DeWames, R. E.; Loyd, C. M. *J. Mol. Spectrosc.* **1962**, *8*, 285−299.

(45) Katriel, J. *J. Phys. B: Atom. Mol. Phys.* **1970**, *3*, 1315−1320.

(46) Cornil, J.; Beljonne, D.; Shuai, Z.; Hagler, T. W.; Campbell, I.; Bradley, D. D. C.; Brédas, J. L.; Spangler, C. W.; Müllen, K. *Chem. Phys. Lett.* **1995**, *247*, 425−432.

(47) Innes, K. K. In *Excited States*; Lim, E. C., Ed.; Academic Press: New York, 1975; Vol. 2; pp 1−32.

(48) Cornil, J.; Beljonne, D.; Heller, C. M.; Campbell, I. H.; Laurich, B. K.; Smith, D. L.; Bradley, D. D. C.; Müllen, K.; Brédas, J. L. *Chem. Phys. Lett.* **1997**, *278*, 139−145.

(49) Oelkrug, D.; Tompert, A.; Gierschner, J.; Egelhaaf, H.-J.; Hanack, M.; Hohloch, M.; Steinhuber, E. *J. Phys. Chem. B* **1998**, *102*, 1902−1907.

(50) de Souza, M. M.; Rumbles, G.; Gould, I. R.; Amer, H.; Samuel, I. D. W.; Moratti, S. C.; Holmes, A. B. *Synth. Met.* **2000**, *111−112*, 539−543.

(51) Ichino, Y.; Ni, J. P.; Ueda, Y.; Wang, D. K. *Synth. Met.* **2001**, *116*, 223−227.

(52) Birckner, E.; Grummt, U.-W.; Rost, H.; Hartmann, A.; Pfeiffer, S.; Tillmann, H.; Hörhold, H.-H. *J. Fluoresc.* **1998**, *8*, 73−80.

(53) Birge, R. R. In *Ultrasensitive Laser Spectroscopy*; Kliger, D. S., Ed.; Academic Press: New York, 1983; pp 109−174.

(54) Karabunarliev, S.; Baumgarten, M.; Bittner, E. R.; Müllen, K. *J. Chem. Phys.* **2000**, *113*, 11372−11381.

(55) Karabunarliev, S.; Baumgarten, M.; Müllen, K. *J. Phys. Chem. A* **2000**, *104*, 8236−8243.

(56) Tian, B.; Zerbi, G.; Schenk, R.; Müllen, K. *J. Chem. Phys.* **1991**, *95*, 3191−3197.

(57) Demas, J. N. *Excited State Lifetime Measurements*; Academic Press: New York, 1983.

(58) van Hutten, P. F.; Krasnikov, V. V.; Hadziioannou, G. *Acc. Chem. Res.* **1999**, *32*, 257−265.

(59) Beljonne, D.; Shuai, Z.; Pourtois, G.; Brédas, J. L. *J. Phys. Chem. A* **2001**, *105*, 3899−3907.

(60) Liu, M. S.; Jiang, X.; Jen, A. K.-Y. *Mater. Res. Soc. Symp. Proc.* **2000**, *598*, BB5.53.1−BB5.53.8.

(61) The values reported in Table 2 and Figure 3 were obtained using fluorescein as the two-photon reference material. When coumarin 307 is used, the two-photon spectra exhibit similar trends, but the magnitude of the cross sections is systematically lower (by about 20%), due to the experimental uncertainty associated with the original literature measurements for the two references. The δ values reported here for molecule **2** differs from a previous determination[8] (δ = 1940 GM with nanosecond pulses and 3670 GM using femtosecond pulses) and reflects the most recent measurements performed in our laboratory.

(62) Kogej, T.; Beljonne, D.; Meyers, F.; Perry, J. W.; Marder, S. R.; Brédas, J. L. *Chem. Phys. Lett.* **1998**, *298*, 1−6.

(63) **1c′** and **3c′** are thus acting as model compounds for **2** and **4**, although the effects of the different substituents on the amino end groups was not accounted for.